Deciphering Potential Chemical Compounds of Gaseous Oxidized Mercury in Florida, USA

Jiaoyan Huang[1], Matthieu B. Miller[2], Eric Edgerton[3], Mae Sexauer Gustin[2]

[1] Institute for the Environment, University of North Carolina, Chapel Hill, 100 Europa Drive, Suite 490, Chapel Hill, NC, 27517, United States

[2] Department of Natural Resources and Environmental Sciences, University of Nevada-Reno,1664 N. Virginia Street, Reno, NV, 89557, United States

[3] Atmospheric Research & Analysis, Inc., 410 Midenhall Way, Cary, North Carolina 27513, United States

12   **Abstract**

13   The highest mercury (Hg) wet deposition in the United States of America (USA) occurs

14   along the Gulf of Mexico, and in the southern and central Mississippi River Valley.

15   Gaseous oxidized Hg (GOM) is thought to be a major contributor due to high water

16   solubility and reactivity. Therefore, it is critical to understand concentrations, potential

17   for wet and dry deposition, and GOM compounds present in the air. Concentrations and

18   dry deposition fluxes of GOM were measured and calculated for Outlying Landing Field

19   (OLF), Florida, using data collected by a Tekran® 2537/1130/1135, the University of

20   Nevada-Reno Reactive Mercury Active System (UNRRMAS) with cation exchange and

21   nylon membranes, and Aerohead samplers that use cation-exchange membranes to

22   determine dry deposition. Relationships with Tekran® derived data must be interpreted

23   with caution, since GOM concentrations measured are biased low depending on the

24   chemical compounds in air, and interferences with water vapor and ozone. Criteria air

25   pollutants were concurrently measured.

26   This allowed for comparison and better understanding of GOM. In addition to other

27   methods previously applied at OLF, use of the UNRRMAS provided a platform for

28   determination of the chemical compounds of GOM in the air. Results from nylon

29   membranes with thermal desorption analyses indicated 7 GOM compounds in this area,

30   including $HgBr_2$, $HgCl_2$, HgO, Hg-nitrogen and sulfur compounds, and two unknown

31   compounds. This indicates that the site is influenced by different gaseous phase reactions

32   and sources. Using back trajectory analysis during a high GOM event related to high CO,

33   but average SO_2, indicated air parcels moved from the free troposphere, and across

34   Arkansas, Mississippi, and Alabama at low elevation (<300 m). This event was initially

35   characterized by $HgBr_2$ followed by a mixture of GOM compounds. Overall, GOM

36   chemistry indicates oxidation reactions with local mobile source pollutants, and long

37   range transport.

38   In order to develop methods to measure GOM concentrations and chemistry, and model

39   dry deposition processes, the actual GOM compounds need to be known, as well as their

40   corresponding physicochemical properties, such as Henry's Law constants.

41   *Keywords: multiple-resistance model, dry deposition, cation exchange membrane,*

42   *criteria pollutants, active samplers*

43

1 Introduction

Mercury (Hg) has been classified as a persistent, bioaccumulative toxin (PBT) (UNEP, 2013), and deposition from the atmosphere is considered the dominant pathway by which Hg enters remote ecosystems (Lindberg et al., 2007). In some areas, scavenging by precipitation controls atmospheric Hg removal processes, such as in the Southeastern United States of America (USA), where precipitation amounts are high (Prestbo and Gay, 2009). However, wet deposition concentrations are not necessarily correlated with precipitation amounts >81mm, and deposition has not decreased with emission reductions as coal combustion facilities in the region have implemented control technologies (Prestbo and Gay, 2009; MDN, 2014). For example, concentrations at OLF 17.1 $\mu g/m^2$ in 2012 and 21.0 $\mu g/m^2$ in 2014 (MDN, 2014). A contributing factor to wet deposition in the Gulf Coast area may be related to high atmospheric convection during thunderstorms and scavenging of gaseous oxidized Hg (GOM) from the free troposphere (Nair et al., 2013), and down mixing of air with high GOM from the free troposphere (Gustin et al., 2012).

An additional concern is that the Tekran® system measurement currently used to quantify GOM does not equally quantify all GOM forms, and has interferences with water vapor and ozone (cf. Ambrose et al., 2013; Gustin et al., 2013; Huang et al., 2013; Lyman et al., 2010; McClure et al., 2014; Lyman et al., 2016). Since GOM is considered an important form that can be rapidly removed from the atmosphere due to high water solubility (Lindberg et al., 2007); it is important to understand both atmospheric concentrations and chemistry (i.e. specific chemical compounds). Use of the University of Nevada-Reno Reactive Mercury Active System (UNRRMAS) that collects GOM on nylon membranes in tandem with cation exchange membranes has indicated that there are different chemical compounds in the air and concentrations are 2-to-13 times higher than previously thought at locations in the Western USA (Huang et al., 2013; Gustin et al., 2016).

Mercury has been studied in Florida for many years, initially because of the high concentrations measured in fish and the Florida Panther (Dvonch et al., 1999; Gustin et al., 2012; Marsik et al., 2007; Pancras et al., 2011; Peterson et al., 2012). Long-term

4

74   GEM and GOM concentrations as measured by the Tekran® system have declined;

75   however, PBM concentrations increased after 2009 (Edgerton, unpublished data),

76   suggesting the atmospheric chemistry has changed. Peterson et al. (2011) and Gustin et al.

77   (2012) suggested based on detailed assessment of passive sampler and Tekran® system

78   collected Hg data, criteria air pollutants, and meteorology that at 3 locations in Florida

79   (OLF, Davie, Tampa) different GOM compounds were present, and these were generated

80   by *in situ* oxidation associated with pollutants generated by mobile sources, indirect and

81   direct inputs of Hg from local electricity generating plants, and direct input of Hg

82   associated with long range transport. At OLF, background deposition was equal to that

83   associated with mobile sources, and a significant component was derived from long range

84   transport in the spring. Long range transport has been reported for OLF in the spring

85   (Weiss-Penzias et al. 2011; Gustin et al., 2012). Long range transport of ozone is a very

86   common event in the spring (see special issues on ozone (Gertler and Bennett, 2015;

87   Lefohn and Cooper, 2015).

88

89   In this work, GOM collected using the UNRRMAS, and the Aerohead dry deposition

90   measurement method (Lyman et al., 2007; 2009) were analyzed, along with Tekran® Hg

91   and criteria air pollutant data to understand GOM chemistry and dry deposition at

92   Outlying Landing Field (OLF), located ~ 15 kilometers NW of Pensacola, Florida.

93   GOM dry deposition fluxes were calculated using deposition velocities determined using

94   a multi-resistance model with ambient air GOM concentrations from the Tekran®

95   system (multiplied by a factor of 3 due to bias in the Tekran® system; cf. Huang and

96   Gustin, 2015), and compared to those obtained using Aerohead data. Chemistry of GOM

97   compounds was identified. Results were used to estimate dry deposition velocities for the

98   GOM compounds observed. The hypothesis for this work was that since GOM

99   compounds can vary spatially and temporally, due to different compounds produced by

100 different sources and processes, this will result in different dry deposition velocities and

101 dry deposition flux.

102 **2 Methods**

103   2.1 Field site

104   The sampling site was located at OLF (30.550°N, 87.374°W, 44 m above sea level). The

105   closest major Hg emission source is a coal-fired power plant (Plant Crist) northeast of the

106   site (Figure 1). This area has been used for atmospheric Hg research in previous studies

107   (Caffrey et al., 2010; Lyman et al., 2009; Gustin et al., 2012; Peterson et al., 2012; Weiss-

108   Penzias et al., 2011). OLF is a coastal site (~25 km away from Gulf of Mexico)

109   influenced by sea breezes especially during the summer (Gustin et al., 2012). Based on

110   cluster analyses of data from one year at this location, ~24% of the air is derived from the

111   marine boundary layer during the day and 60% at night (Figure 1).

112   2.2 Sampling Methods

113   Aerohead samplers for determination of dry deposition were deployed bi-weekly from

114   June 2012 to March 2014. UNRRAMS samples were taken bi-weekly from March 2013

115   to March 2014. Atmospheric Hg concentrations, including GEM, GOM, and PBM, were

116   measured using a Tekran® system (model 2357/1130/1135, Tekran® Instrument Corp.,

117   Ontario, Canada) that was operated with one-hour sampling and one-hour desorption with

118   detection limits of 0.1 ng m^{-3}, 1.5 pg m^{-3}, and 1.5 pg m^{-3}, respectively.

119   Reactive Hg (GOM + PBM) concentrations were measured using the UNRRAMS with 3

120   sets of two in-series 47 mm cation-exchange membranes (ICE450, Pall Corp., MI, USA).

121   Three sets of nylon membranes (0.2 µm, Cole-Parmer, IL, USA) were also deployed to

122   assess Hg compounds in the air (see Pierce and Gustin, 2016 for schematic). Cation

123   exchange membranes have been demonstrated to quantitatively measure specific

124   compounds of GOM in the laboratory; however, may not measure all compounds (Gustin

125   et al., 2015; Gustin et al., 2016). These membranes have also been shown to retain

126   compounds loaded for 3 weeks (Pierce and Gustin, 2016). Nylon membranes do not

127   retain GOM compounds quantitatively, and retention during transport needs to be tested

128   (Huang et al., 2013; Gustin et al., 2015; Gustin et al., 2016). Nylon membrane retention is

129   impacted by relative humidity that might limit uptake of specific forms. Criteria air

130   pollutants and meteorological data, including CO, SO_2, O_3, $PM_{2.5}$, NO, NO_2, NO_y,

131   temperature, relative humidity, wind speed, wind direction, pressure, solar radiation, and

132 precipitation were available at this site for the sampling period. See Peterson et al. (2012)

133 for detailed information on collection of these measurements.

134 Aeroheads and membranes were prepared at UNR, packed in a thermal isolated cooler,

135 and shipped back and forth between the laboratory and site. Samples were stored in a

136 freezer (-22°C) at UNR until analyzed. Cation-exchange membranes were digested and

137 analyzed following EPA Method 1631 E (Peterson et al., 2012), and nylon membranes

138 were first thermally desorbed, and then analyzed using EPA Method 1631 E (Huang et al.,

139 2013). Cation-exchange membrane blanks for Aerohead and UNRRAMS were 0.40±0.18

140 (n=42), 0.37±0.26 (n=77) ng, respectively; and for nylon membranes used in the active

141 system blanks were 0.03±0.03 (n=69) ng. Therefore, method detection limits (MDL, 3-

142 sigma) for two-week sampling time (336 hrs) was 0.13 ng m^{-2} hr^{-1} for dry deposition,

143 respectively. For the active membrane system, the Hg amount on the back-up filters and

144 blanks were not significantly different (cation-exchange membrane: 0.4±0.3 vs 0.4±0.3

145 ng; nylon membrane: 0.03±0.03 vs 0.02±0.02 ng); therefore, the back-up filters were

146 included in the calculation of the bi-weekly blanks. The bi-weekly MDL (336 hrs) for

147 active system with cation-exchange and nylon membranes were 2-68 pg m^{-3}(mean: 24 pg

148 m^{-3}) and 0.01-14.6 pg m^{-3}(mean: 2.1 pg m^{-3}), respectively. Bi-weekly MDL was

149 calculated from 3 times the standard deviation of bi-weekly blanks. The MDL was

150 calculated for each period of sampling, due to the fact this can vary based on treatment of

151 the membranes, when preparing samples for deployment, deployment at the field site,

152 and handling once returned to the laboratory. The membranes may also vary by material

153 lot. All samples were corrected by subtracting the blank for the corresponding two-week

154 period.

155 2.3 Data analyses

156 Hourly Tekran®, criteria air pollutants, and meteorological data were managed and

157 validated by Atmospheric Research & Analysis, Inc (see Peterson et al., 2012). These

158 were then averaged into two-week intervals to merge with the membrane measurements.

159 In previous studies, scaling factors similar to HNO$_3$ ($\alpha=\beta=10$) were used to calculate

160 oxidized Hg dry deposition velocity (Marsik et al., 2007; Castro et al., 2012); however,

161   Lyman et al. (2007) used the effective Henry's Law constant, and half-redox reactions in

162   neutral solutions of $HgCl_2$, and indicated HONO might better represent the chemical

163   properties of oxidized Hg rather than HNO_3. Huang et al. (2015a) indicated that due to

164   limited understanding of oxidized Hg chemical properties, no single value can be used to

165   calculate oxidized Hg dry deposition, because α and β would change with different GOM

166   compounds. Here dry deposition was calculated using the multiple resistance model of

167   Lyman et al. (2007) using both $\alpha=\beta=2$, 5, 7, and 10.

168   Back trajectories were calculated using the Hybrid Single Particle Lagrangian Integrated

169   Trajectory (HYSPLIT 4.9) with EDAS 40-km, 1000-meter starting height. For day and

170   nighttime analyses, starting times were Local Standard Time (LST) 1100-1300 h and

171   100-300 h, 72-hour simulations. For a high-concentration event analyses, trajectories

172   were started for each day at 0000, 0400, 0800, 1200, 1600, and 2000 LST. Overall, the

173   uncertainties of back trajectories calculated from HYSPLIT are 20% of the air parcel

174   traveling distance (Draxler, 2013 ; Gebhart et al., 2005; Stohl, 1998; Stohl et al., 2003).

175   Back trajectories for the entire sampling time were analyzed using cluster analysis (Liu et

176   al., 2010).

177   Sigmaplot 14.0 (Systat Software Inc, San Jose, CA, USA), and Minitab 16.0 (Minitab

178   Inc., PA, US) were used to do t-tests and correlation analyses. Comparisons were

179   considered significantly different and correlations considered significant when $p < 0.05$.

180   **3 Results and Discussion**

181   <u>3.1 Overall measurements</u>

182   Similar to previous work at this location (Gustin et al., 2012), O_3 was highest in the

183   spring; and CO concentrations were high in winter due to a low boundary layer and

184   biomass burning, and low in summer (Table 1). Observations from the 3 GOM sampling

185   methods (Tekran®, and nylon and cation exchange membranes) showed higher GOM

186   concentrations in spring relative to other seasons (Table 1). Concentrations of GOM

187   measured by cation-exchange membranes in the active system were significantly (p-value

188   < 0.05, paired-t test) higher than those measured by Tekran® KCl-coated denuder and

8

189   nylon membranes, both of which have been reported to be influenced by relative

190   humidity (Huang and Gustin, 2015b; Gustin et al., 2015). Mean cation-exchange

191   membrane concentrations were higher than Tekran® derived GOM by 14, 48, 11, and 13

192   times in the spring, summer, fall and winter, respectively.

193   Nylon membranes collected higher GOM concentrations than those measured by the

194   Tekran® in spring 2013 when the humidity was low. Overall, air concentrations

195   measured by the Tekran® system in this study were similar to those measured at OLF in

196   2010 (Peterson et al., 2012). Particulate-bound Hg had the same diel trend as GOM, but

197   higher concentrations.

198   Understanding the oxidants present in air is important for understanding potential GOM

199   compounds. Oxidants to consider include O_3, halogenated compounds, and sulfur and

200   nitrogen compounds (cf. Gustin et al., 2016). Since the active system is currently limited

201   to a 2-week sampling period, they are useful for understanding the specific compounds

202   that might be present, and this in turn can be used to understand sources.

203   3.2 Potential GOM compounds

204   Standard desorption profiles for GOM compounds obtained by Huang et al. (2013) and

205   Gustin et al. (2015) are compared to those obtained at OLF (Figure 2). Compounds used

206   in the permeation tubes included $HgBr_2$, $HgCl_2$, $HgN_2O_6 \cdot H_2O$, $HgSO_4$, and HgO. $HgCl_2$

207   and $HgBr_2$ have been identified as being released from permeation tubes (Lyman et al.,

208   2016); however, the exact N and S compounds are not known. During 10 periods the

209   nylon membranes (collected in triplicate) collected a significant amount of GOM based

210   on their bi-weekly detection limit (Figure 2), and the desorption profiles varied. Although

211   data are limited, we have observed similar thermal desorption compounds in other studies

212   (i.e. Huang et al, 2013 and Gustin et al. 2016). For example, in the marine boundary layer

213   in Santa Cruz, California,based on the additional curves in Gustin et al. (2015), Hg-

214   nitrogen and sulfur compounds were observed. At the Reno Atmospheric Mercury

215   Intercomparison eXperiment site (RAMIX) site, Nevada, Huang et al. (2013) reported

216    $HgBr_2/HgCl_2$ compounds, this is due to free troposphere inputs at this site (Gustin et al.,

217   2013). At a highway impacted site Huang et al. (2013) reported similar patterns to that in

218   Gustin et al. (2016) that included Hg-nitrogen and sulfur compounds, and unknown

219   compounds that generated a high residual tail in the profile. This indicates similar

220   chemical forms are being collected, and is supported by work described below, and that

221   the compounds are not being generated on the membranes. Lack of generation on

222   membranes has also been shown to be the case in a limited study (Pierce and Gustin,

223   2016). In addition to our work, $HgBr_2$ and $HgCl_2$ were reported to occur in Montreal,

224   Canada (Deeds et al., 2015).

225

226   Seven distinct patterns of release were observed from membranes collected at OLF

227   during thermal desorption. One had a high residual tail that does not match our standard

228   profiles; however, was also observed in Nevada (Gustin et al, 2016). These occurred on

229   4/2/2013, 4/9/2013 and 5/21/2013. This suggests that in spring there is a compound that

230   is unknown based on current standard profiles. Based on our methylmercury profile

231   generated using methylmercury added as a liquid to membranes, presented in Gustin et al.

232   (2015), it is possible this could be some organic compound. A nitrogen-based compound

233   was found on 5/21/2013 based on the desorption profile. A pattern occurred on 3/19/2013

234   and 11/19/2013, and this corresponded to $HgBr_2$/$HgCl_2$ with some residual tail that is

235   again some compound not accounted for.

236

237   Patterns observed on 5/7/2013 and 8/27/2013 corresponded to a Hg-nitrogen based

238   compound with a residual tail. The 5th pattern occurred on 1/14/2014, and 9/24/2013 was

239   associated with $HgSO_4$ and the error bars are small. Data collected on 10/22/23 was noisy

240   and had subtle peaks that correspond with HgO, a nitrogen-based compound, and a high

241   residual tail. It is interesting to note that the 11/19 profile was similar to $HgCl_2$.

242   Previous studies reported consistent desorption profiles from 3 sites in Nevada and

243   California without significant point sources (Huang et al., 2013). Huang et al. (2013)

244   presented desorption profiles from a highway, agriculture, and marine boundary layer site.

245   Profiles from the marine boundary layer and agriculture impacted site did not show clear

246   residual tails at 185ºC, but these were observed at the highway impacted site. At OLF, a

247   significant amount of GOM (15-30%) was released after 160 ºC. This and previous work

248   implies that we are missing one or more GOM compound(s) (Figure 2) in our permeation

249 profiles. Interestingly, a peak was found in the 4/9/2013 sample at the GEM release

250 temperature, and this is not due to GEM absorption as demonstrated by Huang et

251 al.(2013), and was also observed in Nevada (Gustin et al., 2016), suggesting an additional

252 unidentified compound. This information indicates GOM compounds at OLF varied with

253 time, and this variation is due to complicated Hg emission sources and chemistry at this

254 location (cf. Gustin et al., 2012).

255 At OLF, GOM composition on the nylon membrane was more complicated than that

256 collected at rural sites in the Western USA (cf. Huang et al.,2013; Gustin et al., 2016);

257 however, similar complexity was observed at a highway location in Reno, Nevada

258 (Gustin et al., 2016). Desorption curves from the nylon filters collected at rural locations

259 in Nevada were in the range of the standard GOM compounds that have been investigated

260 (Huang et al., 2013: Gustin et al., 2016). Curves with multiple peaks in this study imply

261 that there were at least 7 GOM compounds collected on the nylon membranes.

262 3.3 Dry deposition measurements

263 Dry deposition of GOM measured by Aerohead samplers ranged from 0 to 0.5 ng m^{-2} hr^{-1},

264 and 83% of GOM dry deposition was higher than the detection limit (0.13 ng m^{-2} hr^{-1}).

265 Higher GOM dry deposition was observed in spring relative to winter (ANOVA one-way

266 rank, p-value < 0.01); GOM dry deposition was slightly lower in summer and fall (not

267 statistically different) relative to the spring due to high wet deposition and scavenging

268 processes during these seasons. The pattern in GOM seasonal dry deposition was similar

269 to that reported by Peterson et al. (2012). However, GOM dry deposition rates were

270 significantly higher in this study than 2010 values (0.2 vs 0.05 ng m^{-2} h^{-1}). This is due to

271 the correction of 0.2 ng m^{-2} h^{-1} applied in Peterson et al. (2012) to account for

272 contamination of the Aerohead that has been demonstrated to be unnecessary (Huang et

273 al., 2014). Although, highest GOM dry deposition measured using the Aerohead sampler

274 and GOM concentrations measured using the UNRRAMS were observed in spring 2013,

275 the value in March 2014 was relatively low. In March 2014, atmospheric conditions were

276 more similar to winter than spring, with low temperatures and high CO concentrations.

277 These results are different from those calculated using Tekran® measurements that

278 suggest low GOM concentrations and high deposition velocities, and this is because the

279 denuder measurements are biased low.

280 Modeled GOM dry deposition fluxes were calculated using GOM concentrations

281 measured by the Tekran® system that were multiplied by a factor of three (cf. Huang et

282 al., 2014). In general, measured Hg dry deposition fluxes were similar to those modeled

283 simulations with GOM dry deposition $\alpha=\beta=2$ during winter, spring, and fall (see below;

284 Figure 3). Measured Hg dry deposition was significantly higher than modeled results

285 (both $\alpha=\beta=2$ and 10) in summer and early fall (Figure 3). This indicates there are

286 compounds of GOM in the summer that are poorly collected by the denuder, and this also

287 can help explain the higher wet deposition measured during this season (Prestbo and Gay,

288 2009). Highest deposition was measured during the spring, when the input from long

289 range transport is greatest (Gustin et al., 2012). Figure 3 shows the disparity that occurs

290 by season, and comparing model and measured vales. For example in spring a=b=10

291 significantly overestimates deposition, while in the summer and early fall measured

292 deposition is greater than modeled values.

293 Because of the low GOM concentrations and influence of humidity on the nylon

294 membrane measurements (Huang and Gustin, 2015b), GOM compounds were identified

295 only in one summertime sample as $HgN_2O_6 \cdot H_2O$. During this time, measured GOM dry

296 deposition was ~6 times higher than both modeled results, and considering the Tekran®

297 correction factor of 3, membrane-based $HgN_2O_6 \cdot H_2O$ dry deposition flux was ~18 times

298 higher than the Tekran®-model-based value. Gustin et al. (2015) indicated $HgN_2O_6 \cdot H_2O$

299 collection efficiency on cation-exchange membrane in charcoal scrubbed air was ~ 12.6

300 times higher than on Tekran KCl-coated denuder.

301 However, in May 2013, two samples were dominated by a profile similar to the Hg

302 nitrogen-based compound with lower measured/modeled ratios (2.1-6.0 with Tekran®

303 correction factor). This might be due to ambient air GOM chemistry being dominated by

304 a compound with a different dry deposition velocity, less interference on the denuder

305 surface, or parameters in the dry deposition scheme. In May, GOM concentrations

306 measured by the Tekran® were higher than in summer due to lower wet deposition and

307   mean humidity (Table 1). Therefore, despite the fact that GOM collection efficiency

308   associated with the Tekran and nylon membranes are impacted by environmental

309   conditions, this demonstrates the presence of different compounds in the air. The dry

310   deposition scheme needs Henry's Law constants for determining the scaling factors for

311   specific resistances for different compounds (Lyman et al., 2007; Zhang et al., 2002).

312   Lin et al. (2006) stated that the dry deposition velocity of HgO is 2-times higher than that

313   for $HgCl_2$, due to the different Henry's Law constant. The Henry's Law constants for

314    $HgCl_2$, $HgBr_2$, and HgO presented in previous literature (Schroeder and Munthe, 1998)

315   have high uncertainty, for how these calculations were done is not clear (S. Lyman, Utah

316   State University, personal communication, 2015), and the constants for $HgN_2O_6 \bullet H_2O$ and

317    $HgSO_4$ are unknown. Some researchers considered that GOM is similar to HNO_3

318   ($\alpha=\beta=10$), and some treated GOM as HONO ($\alpha=\beta=2$) (Castro et al., 2012; Lyman et al.,

319   2007; Marsik et al., 2007); however, using the parameters of HNO_3 could overestimate

320   GOM dry deposition velocities due to the differences of effective Henry's law constants

321   ($HgCl_2$: ~10^6 HNO_3: ~10^{13} M atm^{-1}).

322   If the ratios ($HgBr_2$: 1.6, $HgCl_2$:2.4, $HgSO_4$: 2.3, HgO: 3.7, and $HgN_2O_6 \bullet H_2O$: 12.6) of

323   GOM concentrations measured by the Tekran® versus cation-exchange membranes for

324   different GOM permeated compounds (Gustin et al., 2015; Huang et al., 2013) are used

325   to correct Tekran® GOM data in this study, modeled GOM dry deposition (Figure 3) are

326   not correlated with measurements. For example, on 3/9/2013 and 11/19/2013 (Figure 3),

327   GOM was dominated by $HgBr_2$ and $HgCl_2$. Dry deposition of $HgBr_2$ from Aerohead

328   measurements and modeling were close to $\alpha=\beta=10$; however, modeled and measured

329    $HgCl_2$ dry deposition were matched as $\alpha=\beta=2$. Average deposition velocity for $\alpha=\beta=2$

330   was 0.78 cm s^{-1}, and for $\alpha=\beta=10$ is 1.59 cm s^{-1}, if we assume the model is right. There

331   were three samples that were identified as Hg-nitrogen based compounds using nylon

332   membranes; however, the ratios of measurement and modeling $HgN_2O_6 \bullet H_2O$ dry

333   deposition were inconsistent over time. In spring, all modeled $HgN_2O_6 \bullet H_2O$ dry

334   deposition values were much higher than measured values; however, in summer,

335   measured and modeled $HgN_2O_6 \bullet H_2O$ dry deposition were similar as $\alpha=\beta=5$ (Table 2). If

336   you assume the dry deposition measurements made by the surrogate surfaces are accurate

337 then this demonstrates there are different forms that occur over time, and these will have

338 different deposition velocities as suggested by Peterson et al. (2012).

339 3.4 Elevated Pollution Event

340 In spring 2013, there was a time period when high concentrations of O_3, CO, and all Hg

341 measured (Figure 4). Figure 5 shows that during this time air masses traveled west to east

342 across the continent. The air movement pattern is similar to that found in Gustin et al.

343 (2012) for OLF Class 2 events which had low SO_2 concentrations. During this 4-week

344 period, air parcels traveling to OLF were in the free troposphere and descended to the

345 surface (Figure 5). Although there are coal-fired power plants in the upwind area within a

346 500 km range (Figure 1), the low SO_2 concentrations, and elevated CO, O_3, and GOM

347 values were not from fossil fuel combustion. Gustin et al. (2012) also indicated that free

348 troposphere air impacted OLF. The first few endpoints for these trajectories indicate air

349 parcels entered North America at > 1000 m agl; therefore, there was transport of some air

350 measured during this time from the free troposphere. Ozone concentrations were also

351 similar to those measured in Nevada in the free troposphere at this time (Gustin et al.,

352 2014). It is important to note that the back trajectories are only for 72 hours and the ones

353 that subsided to surface levels in the Midwest were traveling fast. This is a common event

354 in the spring that represents free troposphere/stratosphere transport into the Western

355 United States and Florida (Gertler and Bennett, 2015; Lefohn and Cooper, 2015 Weiss-

356 Penzias et al., 2011; Gustin et al., 2012)**.**

357
358 The chemical composition of this event suggests potential input from Asia as previously

359 suggested for three locations in Florida in the spring by Gustin et al. (2012). During this

360 time, based on thermal desorption profiles, $HgBr_2$ was measured initially and then the

361 following profiles obtained showed a gradual increase in GOM with increasing

362 temperature with a high residual tail. This would suggest initial subsidence of air from

363 the stratosphere/troposphere (cf. Lyman et al., 2012) followed by a mixture of polluted

364 air as observed in the Western USA (c.f. VanCuren and Gustin, 2015)

365 **4 Conclusions**

The chemical forms of GOM in the atmosphere at OLF varied by season as suggested by Gustin et al. (2012). Seven potential different GOM compounds were identified at OLF using nylon membranes with thermal desorption analysis, including $HgBr_2$, $HgCl_2$, HgO, Hg-nitrogen and sulfur compounds, and 2 unknown compounds. Given the long sampling time detailed assessment of specific sources is difficult, but the presence of different compounds indicate multiple sources and different GOM chemistry. Comparing modeled and measured Hg dry deposition fluxes also demonstrate there are different forms in air and this will affect dry deposition velocities. In order to measure GOM accurately, we need to know what compounds exist in the atmosphere.

5 Acknowledgements

6 References cited

Ambrose, J.L., Lyman, S.N., Huang, J., Gustin, M.S., Jaffe, D.A., 2013. Fast Time Resolution Oxidized Mercury Measurements during the Reno Atmospheric Mercury Intercomparison Experiment (RAMIX). Environmental Science & Technology 47, 7285-7294.

Belis, C.A., Karagulian, F., Larsen, B.R., Hopke, P.K., 2013. Critical review and meta-analysis of ambient particulate matter source apportionment using receptor models in Europe. Atmospheric Environment 69, 94-108.

Brooks, S., Ren, X., Cohen, M., Luke, W., Kelley, P., Artz, R., Hynes, A., Landing, W., Martos, B., 2014. Airborne Vertical Profiling of Mercury Speciation near Tullahoma, TN, USA. Atmosphere 5, 557-574.

Caffrey, J.M., Landing, W.M., Nolek, S.D., Gosnell, K.J., Bagui, S.S., Bagui, S.C., 2010. Atmospheric deposition of mercury and major ions to the Pensacola (Florida) watershed: spatial, seasonal, and inter annual variability. Atmos. Chem. Phys. 10, 5425-5434.

398 Castell-Balaguer, N., Tellez, L., Mantilla, E., 2012. Daily, seasonal and monthly
399   variations in ozone levels recorded at the Turia river basin in Valencia (Eastern
400   Spain). Environmental Science and Pollution Research 19, 3461-3480.
401 Castro, M.S., Moore, C., Sherwell, J., Brooks, S.B., 2012. Dry deposition of gaseous
402   oxidized mercury in Western Maryland. Science of The Total Environment 417-
403   418, 232-240.
404 Choi, H.-D., Huang, J., Mondal, S., Holsen, T.M., 2013. Variation in concentrations of
405   three mercury (Hg) forms at a rural and a suburban site in New York State. Sci.
406   Total Environ.448, 96-106, 2013.
407 Converse, A.D., Riscassi, A.L., Scanlon, T.M. 2014.Seasonal contribution of dewfall to
408   mercury deposition determined using a micrometeorological technique and dew
409   chemistry. Journal of Geophysical Research-Atmospheres119, 284-292.

410 Deeds, D.A., Ghoshdastidar A., Raofie, F., Guerette, E.A., Tessier, .A, Ariya P.A.2015

411   Development of a Particle-Trap Preconcentration-Soft Ionization Mass
412   Spectrometric Technique for the Quantification of Mercury Halides in Air.
413   Analytical Chemistry 87, 5109-5116

414 Dickerson, R.R ., Rhoads, K.P., Carsey, T.P., Oltmans, S.J., Burrows, J.P., Crutzen, P.J.,
415   1999. Ozone in the remote marine boundary layer: A possible role for halogens.
416   Journal of Geophysical Research: Atmospheres 104, 21385-21395.
417 Draxler, R., 2013. What are the levels of uncertainty associated with back trajectory
418   calculations in HYSPLIT. NOAA.
419 Dvonch, J.T., Graney, J.R., Keeler, G.J., Stevens, R.K., 1999. Use of Elemental Tracers
420   to Source Apportion Mercury in South Florida Precipitation. Environmental
421   Science & Technology 33, 4522-4527.
422 Engle, M.A., Tate, M.T., Krabbenhoft, D.P., Kolker, A., Olson, M.L., Edgerton, E.S.,
423   DeWild, J.F., McPherson, A.K., 2008. Characterization and cycling of
424   atmospheric mercury along the central US Gulf Coast. Applied Geochemistry 23,
425   419-437.
426
427 Gay, D.A., Schmeltz, D., Prestbo, E., Olson, M.L., Sharac, T., Tordon, R., 2013. The
428   Atmospheric Mercury Network: measurement and initial examination of an
429   ongoing atmospheric mercury record across North America. Atmos. Chem. Phys.
430   13, 11339-11349.
431 Gebhart, K.A., Schichtel, B.A., Barma, M.G., 2005. Directional biases in back
432   trajectories caused by model and input data. J. Air Waste Manage. Assoc 55,
433   1649-1662
434 Gertler A, Bennett J. The Nevada Rural Ozone Initiative: A framework for developing an
435   understanding of factors contributing to elevated ozone concentrations in rural
436   and remote environments. Science of the Total Environment 2015; 530: 453-454.
437
438 Gustin, Mae Sexauer, Pierce, Ashley M., Huang, Jiaoyan, Miller, Matthieu B., Holmes,
439   Heather,S., Loria-Salazar, S. Marcela (2016) Evidence for different reactive Hg
440   sources and chemical compounds at adjacent valley and high elevation locations,
441   Environmental Science and Technology, 50: 12225-12231.

442

443 Gustin, M., Weiss-Penzias, P., Peterson, C., 2012. Investigating sources of gaseous
444   oxidized mercury in dry deposition at three sites across Florida, USA.
445   Atmospheric Chemistry & Physics 12, 9201-9219.
446 Gustin, M.S., Huang, J., Miller, M.B., Peterson, C., Jaffe, D.A., Ambrose, J., Finley, B.D.,
447   Lyman, S.N., Call, K., Talbot, R., Feddersen, D., Mao, H., Lindberg, S.E., 2013.
448   Do We Understand What the Mercury Speciation Instruments Are Actually
449   Measuring? Results of RAMIX. Environmental Science & Technology 47, 7295-
450   7306.
451 Gustin, M. S. , Amos, H. A, Huang, J., Miller, M.B., Heidecorn. 2015 Measuring and
452   modeling mercury in the atmosphere: A critical review, Invited paper- Special
453   Issue of Atmospheric Chemistry and Physics. Atmospheric Physics and
454   Chemistry, 15: 5697-2015. doi: 10.5194/acp-15-5697-2015.
455

456 Huang, J., Choi, H.-D., Hopke, P.K., Holsen, T.M., 2010. Ambient Mercury Sources in
457   Rochester, NY: Results from Principle Components Analysis (PCA) of Mercury
458   Monitoring Network Data. Environmental Science & Technology 44, 8441-8445.
459 Huang, J., Gustin, M., 2015a,Uncertainties of Gaseous Oxidized Mercury Measurements
460   Using KCl-coated Denuders, Cation-Exchange Membranes, and Nylon
461   Membranes: Humidity Influences, Environmental Science and Technology,
462   49,432-441
463 Huang, J., Lyman, S.N., Hartman, J.S., Gustin, M.S., 2014. A review of passive sampling
464   systems for ambient air mercury measurements. Environmental Science:
465   Processes & Impacts 16, 374-392.
466 Huang, J., Miller, M.B., Weiss-Penzias, P., Gustin, M.S., 2013. Comparison of Gaseous
467   Oxidized Hg Measured by KCl-Coated Denuders, and Nylon and Cation
468   Exchange Membranes. Environmental Science & Technology 47, 7307-7316.
469 Huang J., Gustin M.S. 2015b Use of passive sampling methods and models to understand
470   sources of mercury deposition to high elevation sites in the Western United States.
471   Environmental Science and Technology, 49 (432-441)DOI 10.1021/es502836w
472 Jackson, J.E., 1991 A User's Guide to Principal Components. Wiley.
473 Johnson, J.E., Gammon, R.H., Larsen, J., Bates, T.S., Oltmans, S.J., Farmer, J.C., 1990.
474   Ozone in the marine boundary layer over the Pacific and Indian Oceans:
475   Latitudinal gradients and diurnal cycles. Journal of Geophysical Research:
476   Atmospheres 95, 11847-11856.
477 Landing, W.M., Caffrey, J.M., Nolek, S.D., Gosnell, K.J., Parker, W.C., 2010.
478   Atmospheric wet deposition of mercury and other trace elements in Pensacola,
479   Florida. Atmos. Chem. Phys. 10, 4867-4877.
480 Landis, M.S., Lewis, C.W., Stevens, R.K., Keeler, G.J., Dvonch, J.T., Tremblay, R.T.,
481   2007. Ft. McHenry tunnel study: Source profiles and mercury emissions from
482   diesel and gasoline powered vehicles. Atmospheric Environment 41, 8711-8724.
483 Landis, M.S., Stevens, R.K., Schaedlich, F., Prestbo, E.M., 2002. Development and
484   Characterization of an Annular Denuder Methodology for the Measurement of
485   Divalent Inorganic Reactive Gaseous Mercury in Ambient Air. Environmental
486   Science & Technology 36, 3000-3009.

487   Lefohn AS, Cooper OR. Introduction to the special issue on observations and source
488   attribution of ozone in rural regions of the western United States Preface.
489   Atmospheric Environment 2015; 109: 279-281.

490   Lin, C.-J., Pongprueksa, P., Lindberg, S.E., Pehkonen, S.O., Byun, D., Jang, C., 2006.
491   Scientific uncertainties in atmospheric mercury models I: Model science
492   evaluation. Atmospheric Environment 40, 2911-2928.
493   Lindberg, S.E., Bullock, R., Ebinghaus, R., Engstrom, D., Feng, X., FItzgerald, W.,
494   Pirrone, N., Prestbo, E., Seigneur, C., 2007. A synthesis of progress and
495   uncertainites in attributing the sources of mercury in deposition. AMBIO 36, 19-
496   32.
497   Liu, B., Keeler, G.J., Timothy Dvonch, J., Barres, J.A., Lynam, M.M., Marsik, F.J.,
498   Morgan, J.T., 2010. Urban-rural differences in atmospheric mercury speciation.
499   Atmospheric Environment 44, 2013-2023.
500   Lyman, Seth; Jones, Colleen; O'Neil, Trevor; Allen, Tanner; Miller, Matthieu; Gustin,
501   Mae; Pierce, Ashley; Luke, Winston; Ren, Xinrong; Kelley (2016) Automated
502   Calibration of Atmospheric Oxidized Mercury Measurements Environmental
503   Science and Technology 50 12921-12927
504
505   Lyman, S.N., Gustin, M.S., Prestbo, E.M., Marsik, F.J., 2007. Estimation of Dry
506   Deposition of Atmospheric Mercury in Nevada by Direct and Indirect Methods.
507   Environmental Science & Technology 41, 1970-1976.
508   Lyman S.N., Gustin, M.S., Prestbo, E.M., Kilner, P.I., Edgerton, E., Hartsell, B. 2009.
509   Testing and Application of Surrogate Surfaces for Understanding Potential
510   Gaseous Oxidized Mercury Dry Deposition. Environmental Science &
511   Technology 43, 6235-6241.

512   Lyman, S.N., Jaffe, D.A., 2012. Formation and fate of oxidized mercury in the upper
513   troposphere and lower stratosphere. Nat. Geosci. 5, 114-117.

514   Lyman, S.N., Jaffe, D.A., Gustin, M.S., 2010. Release of mercury halides from KCl
515   denuders in the presence of ozone. Atmospheric Chemistry & Physics 10, 8197-
516   8204.
517   Marsik, F.J., Keeler, G.J., Landis, M.S., 2007. The dry-deposition of speciated mercury
518   to the Florida Everglades: Measurements and modeling. Atmospheric
519   Environment 41, 136-149.
520   McClure, C.D., Jaffe, D.A., Edgerton, E.S., 2014. Evaluation of the KCl Denuder
521   Method for Gaseous Oxidized Mercury using HgBr2 at an In-Service AMNet Site.
522   Environmental Science & Technology 48, 11437-11444.
523   MDN, 2014 http://nadp.sws.uiuc.edu/MDN/annualmdnmaps.aspx Site updated 2104 visited 13
524   November 2016
525   Nair, U.S., Wu, Y., Holmes, C.D., Ter Schure, A., Kallos, G., Walters, J.T., 2013. Cloud-
526   resolving simulations of mercury scavenging and deposition in thunderstorms.
527   Atmos. Chem. Phys. 13, 10143-10157.
528   NOAA, 2008. Eta Data Assimilation System (EDAS40) Archive Information, Silver
529   Spring, MD.

530 Pancras, J.P., Vedantham, R., Landis, M.S., Norris, G.A., Ondov, J.M., 2011. Application
531 of EPA Unmix and Nonparametric Wind Regression on High Time Resolution
532 Trace Elements and Speciated Mercury in Tampa, Florida Aerosol.
533 Environmental Science & Technology 45, 3511-3518.
534 Peterson, C., Alishahi, M., Gustin, M.S., 2012. Testing the use of passive sampling
535 systems for understanding air mercury concentrations and dry deposition across
536 Florida, USA. Science of The Total Environment 424, 297-307.
537 Pierce, A. M., Gustin, M. S. 2016 Development of a particulate mass measurement
538 system for tracing pollution sources using atmospheric mercury concentrations
539 Environmental Science and Technology accepted.
540 Prestbo, E.M., Gay, D.A., 2009. Wet deposition of mercury in the U.S. and Canada,
541 1996-2005: Results and analysis of the NADP mercury deposition network
542 (MDN). Atmospheric Environment 43, 4223-4233.
543 Schroeder, W.H., Munthe, J., 1998. Atmospheric mercury--An overview. Atmospheric
544 Environment 32, 809-822.
545 Seinfeld, J.H., Pandis, S.N., 2006. Atmospheric Chemistry and Physics. John Wiley &
546 Sons, Inc., Hoboken, New Jersey.
547 Song, F., Shin, J.Y., Jusino-Atresino, R., Gao, Y., 2011. Relationships among the
548 springtime ground–level NOX, O3 and NO3 in the vicinity of highways in the US
549 East Coast. Atmos. Poll. Res. 2, 374-383.
550 Stohl, A., 1998. Computation, accuracy and applications of trajectories - a review and
551 bibliography. Atmospheric Environment 32, 947-966.
552 Stohl, A., Forster, C., Eckhardt, S., Spichtinger, N., Huntrieser, H., Heland, J., Schlager,
553 H., Wilhelm, S., Arnold, F., Cooper, O., 2003. A backward modeling study of
554 intercontinental pollution transport using aircraft measurements. J. Geophys. Res.
555 108, 4370; DOI: 10.1029/2002JD002862
556 VanCuren R, Gustin MS. Identification of sources contributing to PM2.5 and ozone at
557 elevated sites in the western US by receptor analysis: Lassen Volcanic National
558 Park, California, and Great Basin National Park, Nevada. Science of the Total
559 Environment 2015; 530: 505-518.

560 UNEP, 2013. Global Merucry Assessment 2013-Sources, Emissions, Releases, and
561 Environmental Transport. UNEP Division of Technology, Industry and
562 Economics,Chemicals Branch International Environment House
563 Weiss-Penzias, P., Jaffe, D., Swartzendruber, P., Hafner, W., Chand, D., Prestbo, E.,
564 2007. Quantifying Asian and biomass burning sources of mercury using the
565 Hg/CO ratio in pollution plumes observed at the Mount Bachelor observatory.
566 Atmospheric Environment 41, 4366-4379.
567 Weiss-Penzias, P., Jaffe, D.A., McClintick, A., Prestbo, E.M., Landis, M.S., 2003.
568 Gaseous Elemental Mercury in the Marine Boundary Layer:??Evidence for Rapid
569 Removal in Anthropogenic Pollution. Environmental Science & Technology 37,
570 3755-3763.
571 Weiss-Penzias, P.S., Gustin, M.S., Lyman, S.N., 2011. Sources of gaseous oxidized
572 mercury and mercury dry deposition at two southeastern U.S. sites. Atmospheric
573 Environment 45, 4569-4579.
574 Zhang, L., Brook, J.R., Vet, R., 2003. A revised parameterization for gaseous dry
575 deposition in air-quality models. Atmos. Chem. Phys. 3, 2067-2082.

576   Zhang, L., Moran, M.D., Makar, P.A., Brook, J.R., Gong, S., 2002. Modelling gaseous
577   dry deposition in AURAMS: a unified regional air-quality modelling system.
578   Atmospheric Environment 36, 537-560.
579
580
581

582 Table 1 – Overall seasonal average of criteria air pollutants, GEM, PBM, GOM
583 (measured using three different methods) concentration, GOM dry deposition (DD), and
584 meteorological data at OLF.

	2012			2013				2014
	Summer	Fall	Winter	Spring	Summer	Fall	Winter	March
Ozone [ppb]	30±15	30±12	29±11	38±12	24±12	26±11	27±10	35±12
CO [ppb]	143±38	161±35	167±41	165±36	139±35	156±33	167±35	183±33
SO$_2$ [ppb]	0.3±0.4	0.6±1.5	0.4±0.5	0.3±0.5	0.2±0.3	0.4±0.5	0.7±1.2	0.3±0.4
NO [ppb]	0.3±0.7	0.3±0.7	0.3±0.8	0.2±0.5	0.3±0.7	0.3±0.8	0.4±0.8	0.2±0.5
NO$_2$ [ppb]	2.4±2.4	3.0±2.7	3.0±3.1	2.0±2.3	2.2±2.1	3.1±2.9	3.2±3.0	2.3±2.8
NO$_y$ [ppb]	3.6±2.9	4.3±3.1	4.3±3.6	3.1±2.8	3.2±2.5	4.4±3.3	4.2±3.4	3.6±3.1
GEM [ng m^{-3}][a]	1.2±0.1	1.2±0.1	1.3±0.1	1.2±0.2	1.1±0.1	1.0±0.1	1.2±0.3	1.2±0.1
GOM [pg m^{-3}][a]	0.6±1.3	1.1±2.8	1.0±2.2	2.9±5.1	0.5±1.0	1.1±2.1	1.3±2.5	2.0±3.6
PBM [pg m^{-3}][a]	2.4±2.6	3.6±3.8	7.3±8.7	5.9±6.8	2.3±2.0	2.9±2.3	4.9±5.3	4.0±3.4
GOM [pg m^{-3}][b]	-	-	-	43±110	24±57	14±18	17±23	24±15
GOM [pg m^{-3}][c]	-	-	-	4±10	0.4±1.3	1.2±1.1	0.6±0.6	0.6±0.5
GOM DD [ng m^{-2} hr^{-1}]	0.24±0.20	0.17±0.12	0.15±0.06	0.40±0.23	0.20±0.13	0.13±0.18	0.20±0.50	0.14±0.04
WS [m s-1]	2.1±1.2	2.1±1.0	2.8±1.7	2.9±1.8	2.0±1.1	2.1±1.1	2.5±1.3	2.5±1.5
TEMP [°C]	26±3	19±6	14±6	18±6	26±3	20±7	11±7	14±5
RH [%]	83±14	76±18	79±19	73±21	84±13	77±17	76±23	78±21
SR [w m^{-2}]	230±302	193±271	121±199	266±304	210±278	175±255	129±212	182±278
Precipitation [mm]	637	186	385	223	1010	254	357	183

585
586 [a]: Tekran data
587 [b]: cation-exchange membrane data
588 [c]: nylon membrane data
589

21

Table 2 – Modeled (multiple-resistance model) and measured (surrogate surfaces) GOM dry deposition (ng m^{-2} hr^{-1}), GOM concentrations used to calculate for modeled results are from the Tekran® data and corrected by compounds' corresponding ratios from Gustin et al. (2015; 2016). The sample with unknown compound is used the Tekran® data with correction factor of three (average ratio). The tentative GOM compounds are identified from nylon membrane results.

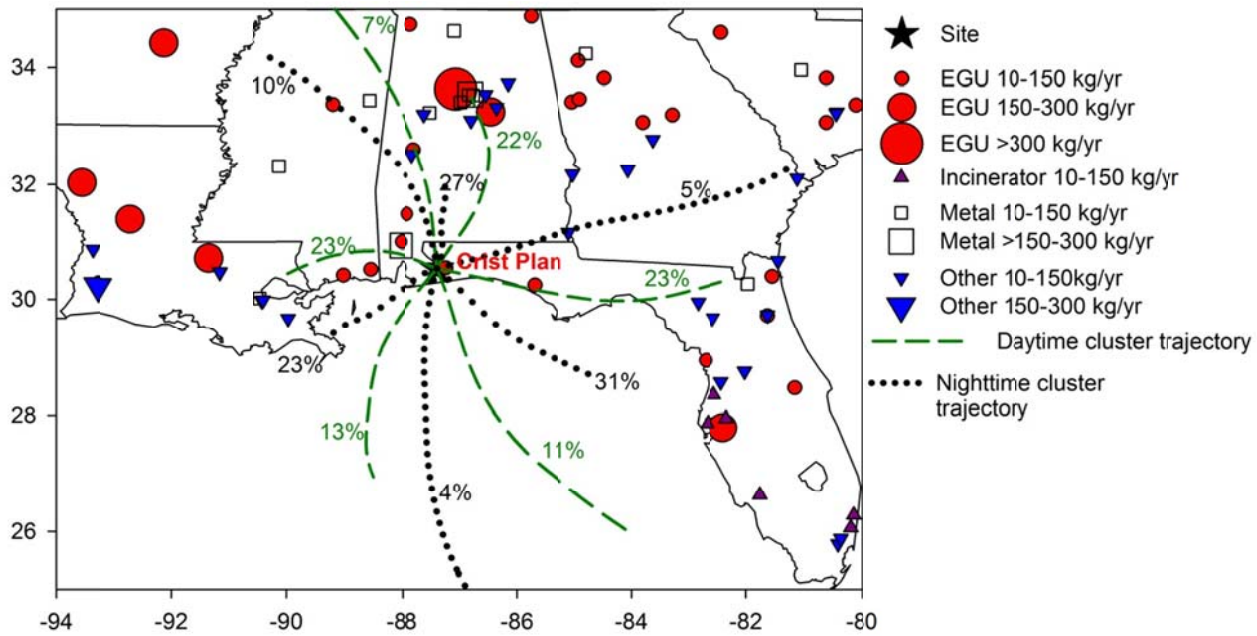| Start date	Tentative GOM compound	Measured GOM dry deposition flux	Modeled GOM dry deposition $\alpha=\beta=2$	Modeled GOM dry deposition $\alpha=\beta=5$	Modeled GOM dry deposition $\alpha=\beta=7$	Modeled GOM dry deposition $\alpha=\beta=10$
3/12/2013	HgBr$_2$	0.50±0.06	0.34	0.49	0.54	0.58
3/26/2013	unknown	0.40±0.11	0.34	0.47	0.52	0.56
4/30/2013	Hg(NO$_3$)$_2$	0.50±0.13	1.21	1.67	1.81	1.95
5/14/2013	Hg(NO$_3$)$_2$	0.40±0.09	1.19	1.69	1.88	2.07
8/20/2013	Hg(NO$_3$)$_2$	0.15±0.07	0.10	0.14	0.16	0.17
11/12/2013	HgCl$_2$	0.08±0.03	0.11	0.16	0.17	0.19
1/7/2014	HgSO$_4$	0.19±0.03	0.18	0.24	0.27	0.29

Figure Caption

Figure 1 – Sampling site and point sources (NEI 2011) map. Cluster trajectories for daytime (11:00-13:00) and nighttime (1:00-3:00).
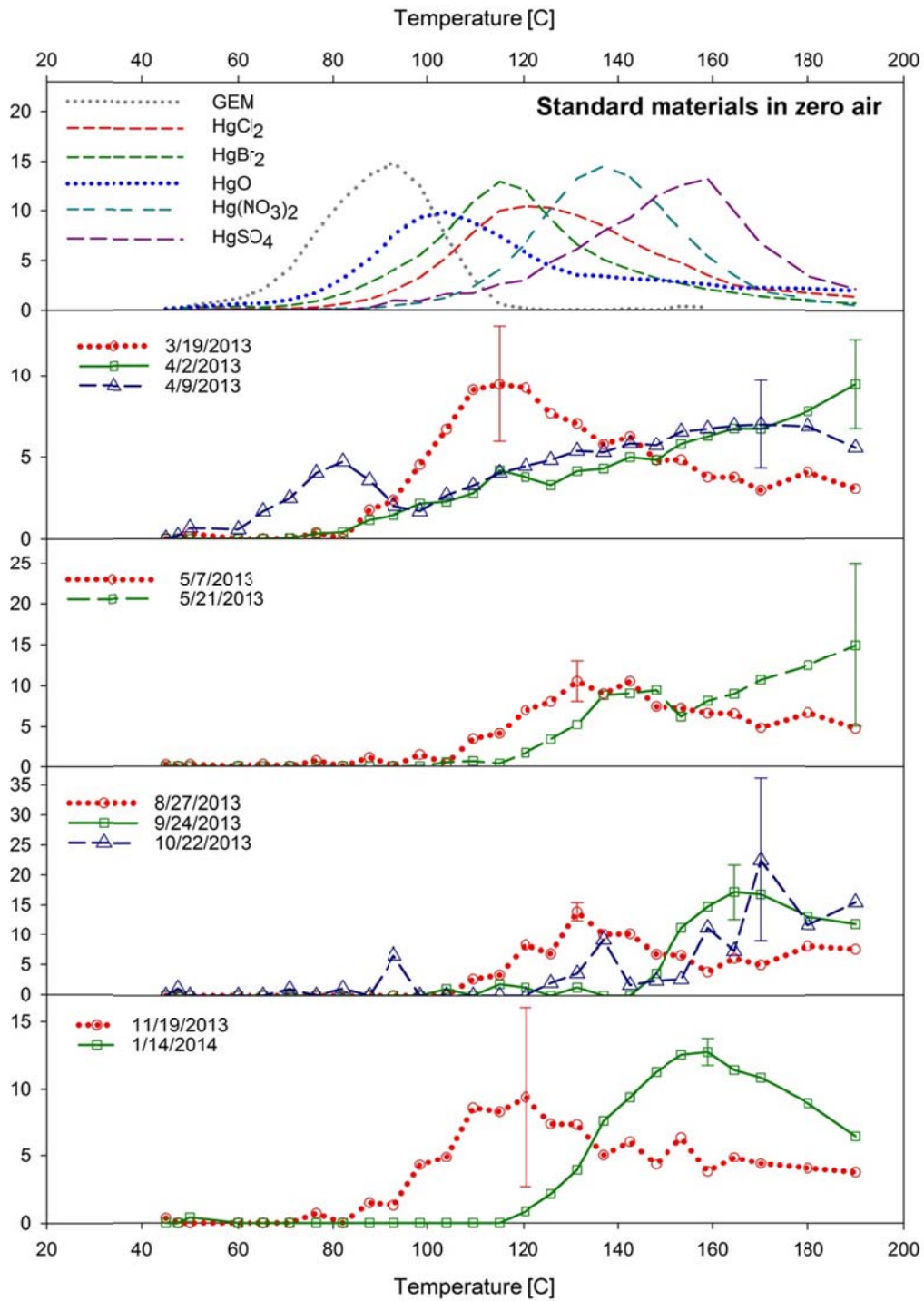
Figure 2 – Desorption profiles from nylon membranes with standard materials in laboratory investigation (top) and field measurements. Whisker is 1 standard variation, and only present in the desorption peak. Note the Hg-nitrogen compound in the permeation tube was $HgN_2O_6 \cdot H_2O$.
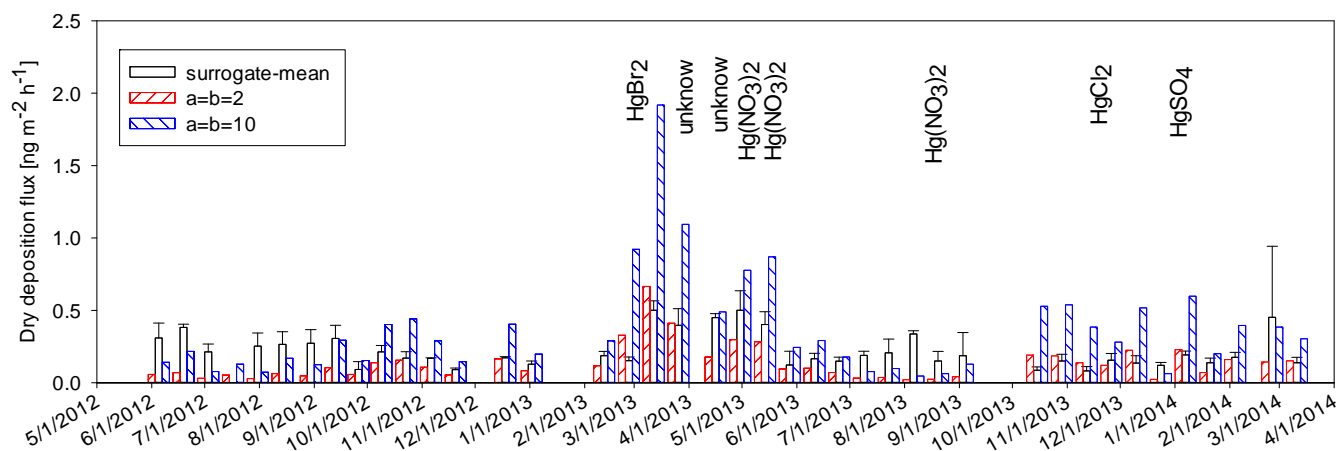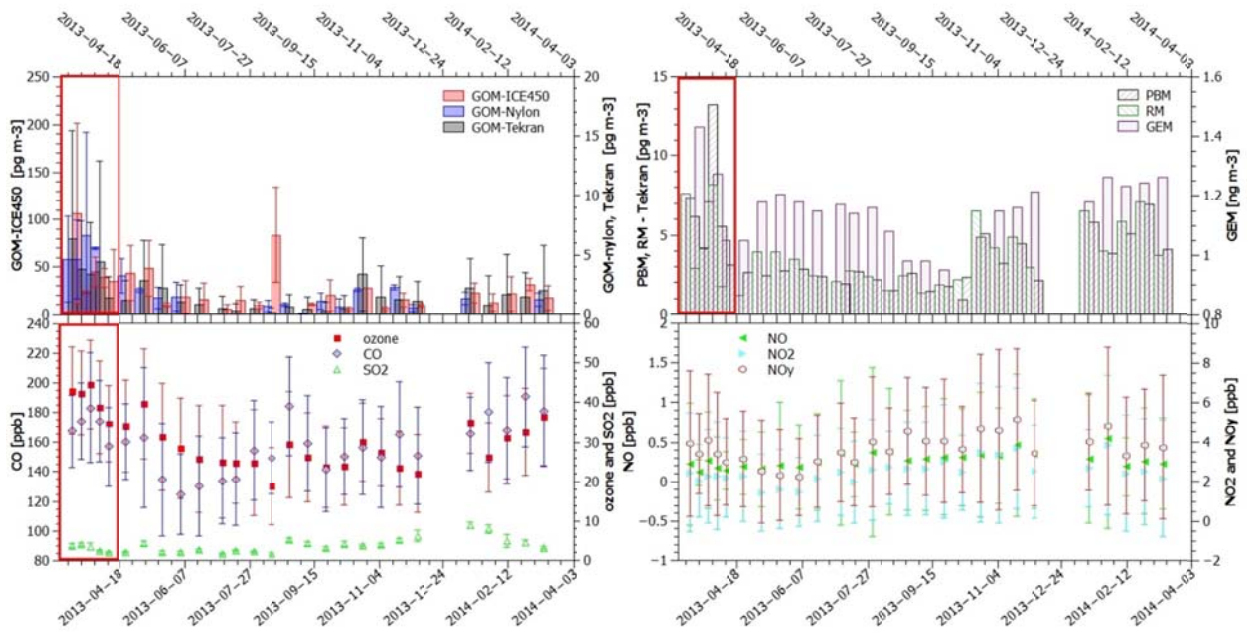
Figure 3 – Measured and modeled GOM dry deposition fluxes, Tekran® data (correction factor of three) were used with multiple resistance models ($\alpha=\beta=2$ and 10). Tentative GOM compounds were determined using the results from nylon membranes desorption.

Figure 4 – Temporal variation of GOM concentrations (mean ± standard deviation, bi-week average), outlined rectangle indicates a polluted event with high Hg, CO, and ozone concentrations. Data are missing for 3 weeks because it was not collected. Tekran data is presented when >75% of the data were available and membrane data are shown when above the method detection limit.
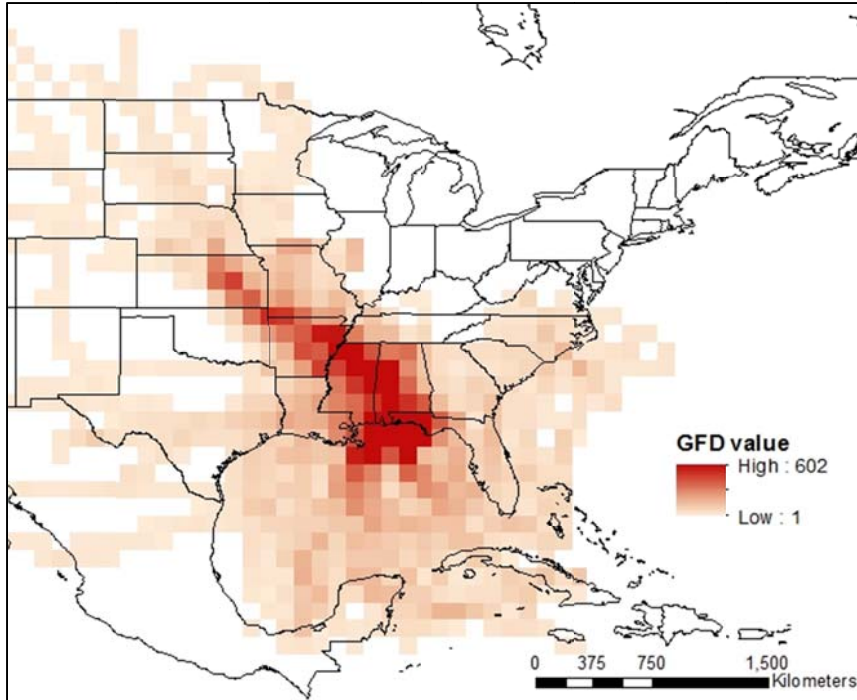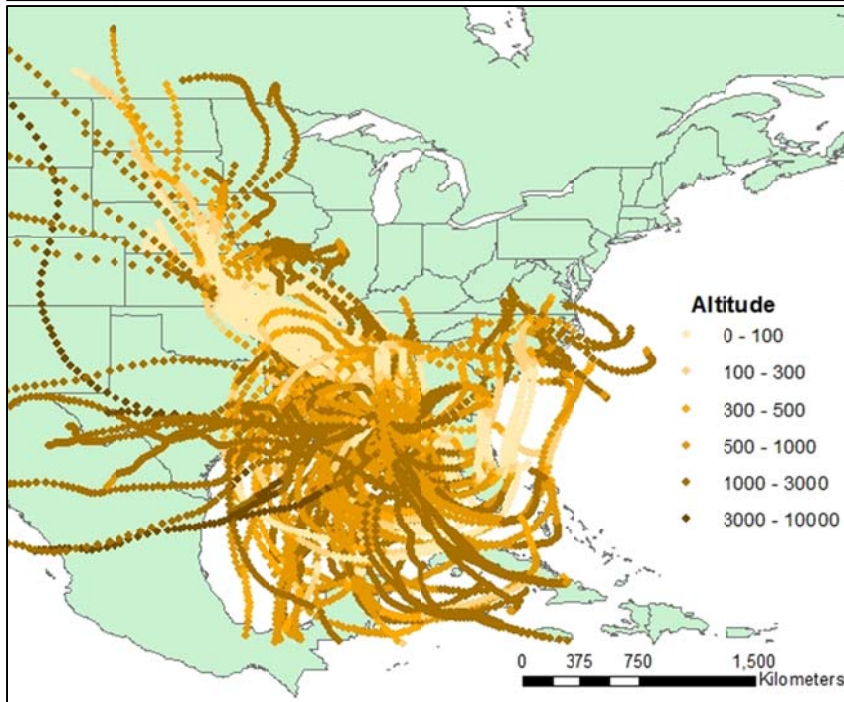
Figure 5 – Results of gridded frequency distribution (top panel), light color indicates less endpoints in a grid. Altitude of 72-hr trajectories (bottom panel) during the polluted event (3/12/2013-4/2/2013), light color of dots on left panel represents low altitude.

Figure 1 – Sampling site and point sources (NEI 2011) map. Cluster trajectories for daytime (11:00-13:00) and nighttime (1:00-3:00).

Figure 2 – Desorption profiles from nylon membranes with standard materials in laboratory investigation (top) and field measurements. Whisker is 1 standard variation, and only present in the desorption peak. Note the Hg-nitrogen compound in the permeation tube was $HgN_2O_6 \cdot H_2O$.

Figure 3 – Measured and modeled GOM dry deposition fluxes, Tekran® data (correction factor of three) were used with multiple resistance models (α=β=2 and 10). Tentative GOM compounds were determined using the results from nylon membranes desorption.

1


2
3 Figure 4 – Temporal variation of GOM concentrations (mean ± standard deviation, bi-week
4 average), outlined rectangle indicates a polluted event with high Hg, CO, and ozone
5 concentrations. Data are missing for 3 weeks because it was not collected. Tekran data is
6 presented when >75% of the data were available and membrane data are shown when above the
7 method detection limit.

8

9

10

11 Figure 5 – Results of gridded frequency distribution (top panel), light color indicates less

12 endpoints in a grid. Altitude of 72-hr trajectories (bottom panel) during the polluted event

13 (3/12/2013-4/2/2013), light color of dots on left panel represents low altitude.

14